Article

Energy consumption of common desktop additive manufacturing technologies

Hopkins, Nicholas, Jiang, Liben and Brooks, Hadley Laurence

Hopkins, Nicholas, Jiang, Liben ORCID: 0000-0003-4686-5942 and Brooks, Hadley Laurence ORCID: 0000-0001-9289-5291 (2021) Energy consumption of common desktop additive manufacturing technologies. Cleaner Engineering and Technology, 2 . ISSN 2666-7908

It is advisable to refer to the publisher's version if you intend to cite from the work.
http://dx.doi.org/10.1016/j.clet.2021.100068

Cleaner Engineering and Technology 2 (2021) 100068

Contents lists available at ScienceDirect

Cleaner Engineering and Technology

journal homepage: www.journals.elsevier.com/cleaner-engineering-and-technology

Energy consumption of common desktop additive manufacturing technologies

Nicholas Hopkins, Liben Jiang, Hadley Brooks *

School of Engineering, University of Central Lancashire, Preston, United Kingdom

ARTICLE INFO

Keywords:
Energy
Additive manufacturing
3D printing
Fused filament fabrication
Vat polymerisation
Prediction

ABSTRACT

Additive manufacturing (AM), also referred as 3D printing, is a small but fast-growing sub-sector of the manufacturing industry. Concerns over increasing worldwide energy consumption provides an impetus to quantify the energy use of the most common forms of AM technologies. To date, research efforts have focussed on the energy use of industrial AM machines, and little research has been conducted on the numerous low-cost desktop 3D printers. Additionally, there is a gap in our knowledge of how to minimise the energy consumption of desktop 3D printers and how to predict their energy use. To fill this gap, high resolution (1 Hz) power measurements were made for a range of low-cost fused filament fabrication and vat polymerisation desktop 3D printers. The volumetric specific energy use was found to be 24.8–85.7 kJ/cm^3 and 10.8–21.5 kJ/cm^3 for fused filament fabrication and vat polymerisation respectively. Semi-empirical equations were developed that can accurately predict the energy use for each printing technology based on simple 3D printing metrics.

1. Introduction

1.1. Background

Global energy consumption is expected to increase for decades to come. The burning of fossil fuels is the main cause of excessive CO_2 emissions within the atmosphere, leading to climate change and sea-level rises. Despite efforts to decarbonise over the last 30 years, 84.7% of total energy use still comes from traditional fossil fuels (Dudley 2019).

The industrial sector is the most significant consumer of energy since 1971, followed by transportation, residential and commercial sectors (International Energy Agency 2019). Additive manufacturing (AM), also known as 3D printing, is a small but fast-growing manufacturing sub-sector with compound annual growth rates of 24.5% (T. Wohlers et al., 2019). AM currently accounts for less than 0.1% of the global manufacturing market; however, there is consensus amongst industry experts that this share will continue to grow, with estimates ranging from 1% to 25% as the sector matures (A. T. Kearney 2018; 3D Hubs 2019). Research into the energy use of AM technologies has historically focussed on industrial, powder-based processes. Baumers, Tuck et al. (2013) discussed the implementation of a tool for the estimation of energy flows occurring in direct metal laser sintering. Meteyer, Xu et al. (2014) presented an energy and material consumption model for binder jetting. Yoon, Lee et al. (2014) compared energy consumption at the process level for conventional and additive manufacturing processes. Jackson, Van Asten et al. (2016) compared the energy requirements for wire-based additive-subtractive hybrid manufacturing and powder-based hybrid additive-subtractive manufacturing. Rejeski, Zhao et al. (2018) outlined the environmental implications of AM, noting that AM uses more energy than comparable conventional manufacturing processes. Yang, Li et al. (2017) measured the energy use of an EnvisionTec MSLA 3D printer and developed a corresponding mathematical model. Peng and Sun (2017) carried out a life cycle assessment for fused deposition modelling however details of the printer and methodology was limited.

Worldwide sales of desktop 3D printers with values under 5000 USD are growing exponentially with over half a million units sold in 2018 alone (T. Wohlers et al., 2019). As the number of desktop 3D printers proliferate, estimating the energy used by these machines becomes increasingly important. This paper aims to address the current lack of energy data, evidence-based energy reduction strategies, and energy prediction models associated with low-cost desktop 3D printers.

This paper has four main aims:

1. Catalogue the energy use of common desktop 3D printers for use in life cycle assessments and other analyses.
2. Assess the effects of a variety of 3D printing parameters on energy consumption.

* Corresponding author.
E-mail addresses: Nhopkins4@uclan.ac.uk (N. Hopkins), lijang2@uclan.ac.uk (L. Jiang), hlbrooks1@uclan.ac.uk (H. Brooks).

https://doi.org/10.1016/j.clet.2021.100068
Received 14 December 2020; Received in revised form 6 February 2021; Accepted 3 March 2021

Abbreviations

AM	Additive Manufacturing
FFF	Fused Filament Fabrication
ME	Material Extrusion
VP	Vat Polymerisation
SLA	Stereolithography Apparatus
MSLA	Masked Stereolithography Apparatus
PLA	Polylactic Acid
TPU	Thermoplastic Polyurethane
PETG	Polyethylene Terephthalate Glycol
PA	Polyamide
VSEC	Specific Energy Consumption

3. Identify effective methods of reducing energy consumption.
4. Develop models for predicting energy use based on simple 3D printing metrics.

The two most common desktop 3D printer categories are (i) fused filament fabrication (FFF), and (ii) vat polymerisation (VP), specifically stereolithography apparatus (SLA) and masked stereolithography apparatus (MSLA).

The energy required to produce the feedstock materials for the printers is considered out of scope of this study.

1.2. Energy theory

FFF printers operate by selectively depositing molten polymer to build parts in successive layers. VP printers work by selectively exposing layers of photopolymer resin with UV light. SLA printers use UV lasers to cure each layer, while MSLA printers use LCD masks and UV lamps/LEDs.

There are two fundamental energy requirements to form parts using FFF or VP technologies: The first is the energy required to move the feedstock material from its locally stored position to its new position in the finished part. This is a small amount of energy due to the short distances involved. The second is the energy required to transform the physical or chemical state of the polymers. All other energy used by the printers, such as that used for heated beds, controllers, fans, overcoming friction and LCD screens should be minimised. The following sections are used to calculate the minimum theoretical energy required to melt or polymerise a unit mass of material. These values can then be used as a lower theoretical limit to help gauge manufacturing efficiency.

1.2.1. Energy required to melt thermoplastics for FFF

FFF operates via the selective deposition of molten polymer to form parts. The energy required to melt m kilograms of polymer is calculated by Eq. (1) where Q = energy (kJ), m = mass of polymer (kg), c = specific heat capacity (kJ/kgK), T_m = polymer melting temperature (°C), T_a = ambient temperature (°C) and H_f = heat of fusion (kJ/kg).

$$Q = mc(T_m - T_a) + mH_f \quad (1)$$

Inputting values for 1 kg of PLA as stated in (Khoo et al., 2016) in Eq. (1) and a melting temperature of 180 °C we get 380 kJ/kg or 475 J/cm^3.

1.2.2. Energy required to polymerise photopolymers for VP

The photopolymerisation process for VP was modelled by (Jacobs 1992). Polymerisation of photopolymer resins depends on two main factors, i.e. the penetration depth of the curing light and the energy required for polymerisation. Jacobs' working curve equation, Eq. (2), describes the relationship:

$$C_d = D_p \ln(E_0 / E_c) \quad (2)$$

Where C_d is the depth/thickness of cured resin (um), D_p is the depth (um) at which the penetrating light intensity falls to 1/e of the surface intensity, E_0 is the energy of light at the surface (mJ/cm^2), and E_c is the "critical" energy required to initiate polymerisation (mJ/cm^2).

Using values of Dp = 192 μm, E_0 = 100 mJ/cm^2 and Ec = 12.6 mJ/cm^2 for Formlabs clear resin cured with 405 nm light (Bennett 2017) we can calculate an approximate minimum energy to cure a cubic centimetre of resin to be 2.5 J/cm^3. Assuming a resin density of 1.15 kg/l then this equates to 2.2 kJ/kg.

Based on this analysis, the minimum energy required to cure a unit mass of photopolymer resin is two orders of magnitude lower than that required to melt an equivalent volume of thermoplastic.

The following section outlines the experimental method used in this study.

2. Experimental method

A single object was designed for the trials to allow a direct comparison of the energy use of a range of 3D printers and print parameters.

2.1. Design of sample parts

The authors recognise that part geometry may impact the amount of energy required to 3D print a unit volume of material. To mitigate the effects of part geometry on specific energy consumption, a custom part (Fig. 1), was designed consisting of three sub-components, with a range of geometric complexities (surface area to volume ratios). The part was also designed to be printed without supports which is common practice for FFFparts.

2.2. Power meter and data logging

A custom power meter/data logger was constructed to allow power to be sampled at 1 Hz with a measurement accuracy of ±1.0%. The data was saved to an SD card. The schematic for the power meter and data logging equipment is shown in Fig. 2.

The current transformer enclosed the live wire of an extension cord between the mains power socket and the printers' power supply unit. The power meter measured both current and voltage allowing power factor corrected readings.

2.3. 3D printing methodology

A range of printers, materials and layer heights were tested, as summarised in Table 1. Room temperature for all printing ranged from 22 to 25 °C.

2.3.1. FFF build parameters

The FFF parts were arranged on the build platform, as shown in Fig. 3. Brims were used to ensure good adhesion to the build surface, and parts were arranged close together to reduce nozzle travel time.

Baseline print settings for the FFF printers are summarised below:

- Nominal print speed 50 mm/s
- Extrusion widths 0.4–0.45 mm
- Brim 5 mm
- 0.4 mm nozzle
- 20% rectilinear infill
- 3 perimeters
- 6 bottom and top layers
- 5 mm retraction

The Geeetech A10M printer is equipped with a 2-into-1 hotend which allowed one of the sub-components to be printed in a different colour to the other components. To purge the hotend between colour changes an

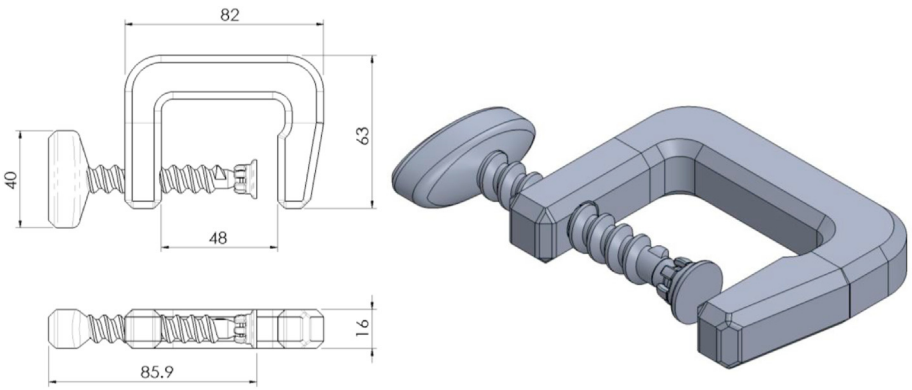

Fig. 1. Assembled G-clamp consisting of three sub-components.

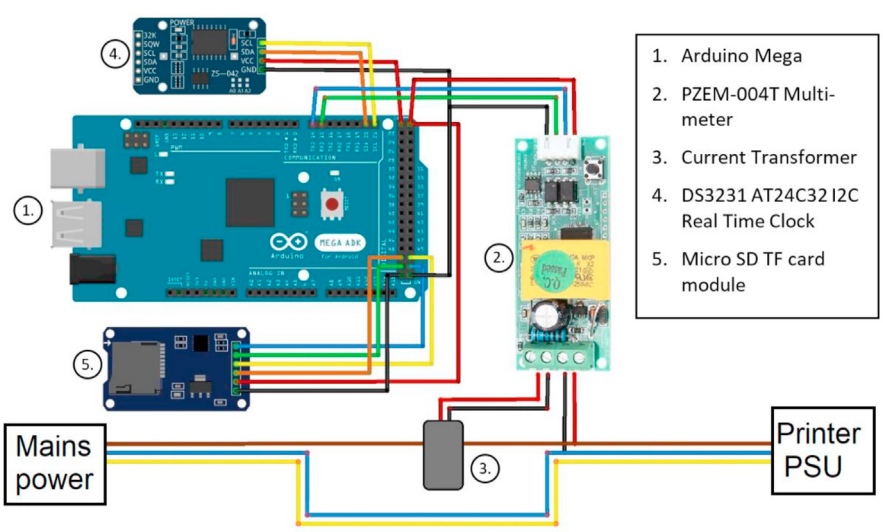

Fig. 2. Schematic for the power meter and data logging equipment.

Table 1
Print combinations.

Printer Category	Printer	Materials	Layer height (μm)
FFF	Creality Ender 3	PLA, TPU, PETG, PA	100, 200, 300
	Geeetech A10M	PLA	200
VP	Formlabs Form1+	Grey resin V2	25, 50, 100
	Anycubic Photon	Anycubic Clear Green resin	50, 75, 100

additional purge block was required.

2.3.2. *Formlabs form 1+ build parameters*

The part orientation and positioning in the Form1+ build volume was done automatically by the algorithms in Preform build preparation software, using the default settings (Fig. 4). The parts were printed solid as VP slicing software does not typically create sparse infill structures. The volume of resin used for each print was 67 mL.

2.3.3. *Anycubic Photon print layout*

The Anycubic Photon slicing software does not have automatic part orientation algorithms, so the parts were orientated similar to the Formlabs prints (Fig. 5). The parts were printed solid with medium support density. The volume of resin used for each print was 66 mL.

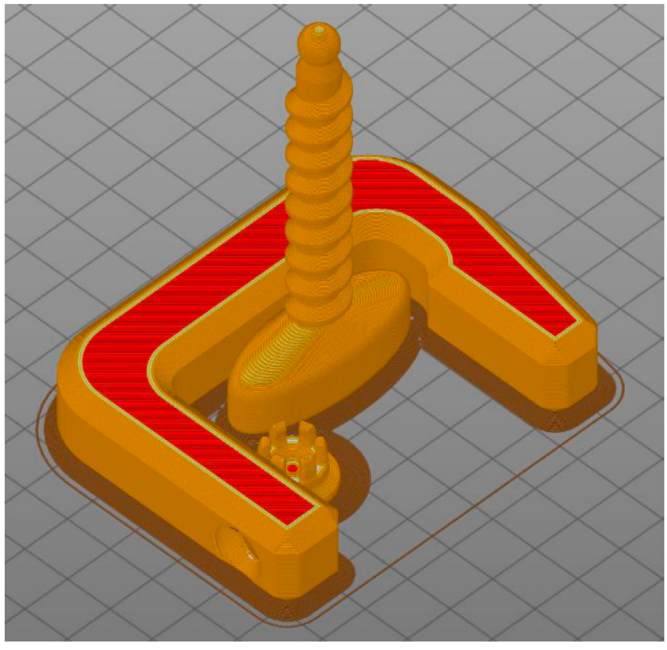

Fig. 3. Print preview of the G-clamp in PrusaSlicer.

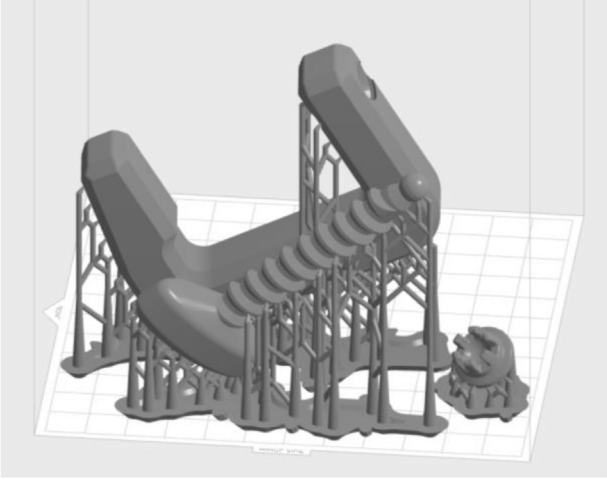

Fig. 4. Print preview in Formlabs Preform.

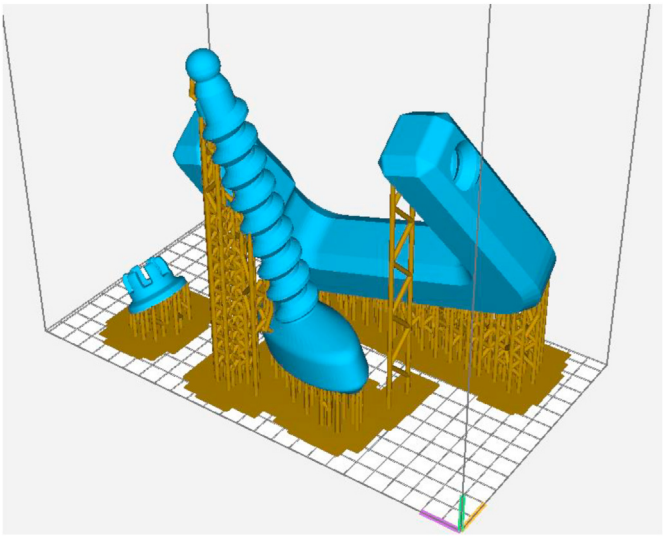

Fig. 5. Print preview in Anycubic Photon Slicer.

The print settings used for the Photon are shown in Table 2.

2.3.4. Post-processing

The FFF prints did not require post-processing, other than removing the brims by hand. The VP prints required washing in isopropyl alcohol to remove excess resin and were post-cured to improve material properties. A Formlabs automated wash station (Form wash) was used with a washing time of 20 min. A Formlabs curing oven (Form cure) was used to fully cure the parts for 60 min at 60 °C.

3. Results and discussion

3.1. Fused filament fabrication (FFF) results

3.1.1. FFF power plots

Fig. 6 shows the raw and smoothed data collected for a PLA print of a G-clamp using the baseline FFF settings. A gaussian weighted moving average with a window length of 180 was used to generate the smoothed trendline. As shown in Fig. 6 the printer rapidly modulates power use by approximately 200 W during operation. Most of this modulation is due to the heated bed turning on and off. The initial peak in power is due to the heated bed warming up. The moving average of power is fairly constant despite large variations in the layer print times over the duration of the print.

Table 2
Print parameters for the Anycubic Photon.

Layer height (μm)	Standard exposure time (s)	Off time (s)	Bottom exposure time (s)	Bottom layers
50	10	1	50	8
75	15	1	50	8
100	20	1	50	8

Fig. 7 shows the first 5 min of the print in more detail. The heating phases of the heated-bed and hotend can be inferred.

3.1.2. FFF layer height comparisons

PLA parts were printed with a range of layer heights to determine the effect of layer height on the volumetric specific energy consumption (VSEC). All other print parameters were kept identical to the baseline print. Varying the layer height was found to change the extruded volume for each part (Table 3). This is likely due to the way the slicer adjusts extrusion widths with layer height and the rounding of part height to the nearest multiple of the layer height.

VSEC values were calculated to allow comparison with polymers of different densities. Logarithmic relationships were found between VSEC, layer height and print time (Fig. 8). The reason the layer heights did not have a linear relationship with print time may be due to volumetric extrusion limits.

3.1.3. Non-baseline FFF prints

To satisfy the secondary aim of the paper, i.e. identifying methods to reduce energy consumption, a variety of print strategies and printer modifications were trialled on the Ender 3 printer. The changes include insulating the heated bed and hotend, printing with no heated bed, sequentially printing each sub-component, printing with 100% infill and ghost printing (running the printer with all the heating elements turned off and no filament). The results are shown in Table 4.

Whilst the 100% infill and multi-colour modes required more energy than the baseline, the VSEC was less due to the higher volume of material printed and a lower proportion of time spent on initial bed heating and non-printing moves (retraction and travel moves) (Fig. 9).

By comparing the energy use of the baseline print with the 'no heated bed' and 'ghost' print modes it is possible to determine the proportion of energy used by the main components of the printer. Fig. 10 shows that over half of the energy is used by the heated bed, while the controller and motion system use 19%. When printing a high-temperature material like nylon the energy fractions for the hotend and heated bed will increase,

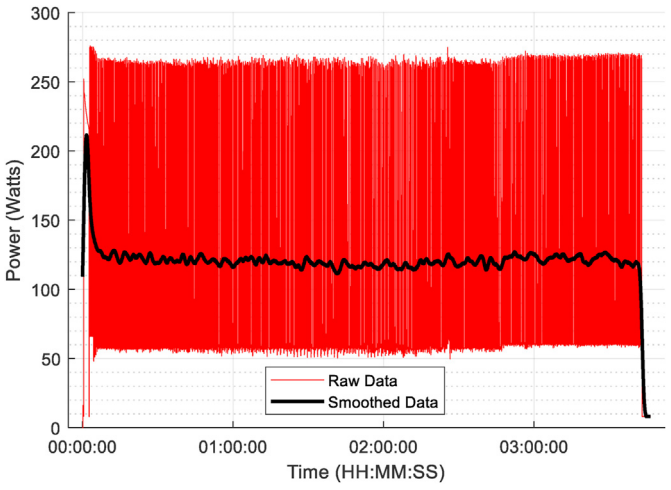

Fig. 6. Measured power over time for a PLA, 0.2 mm layer height print on a stock Ender 3 printer.

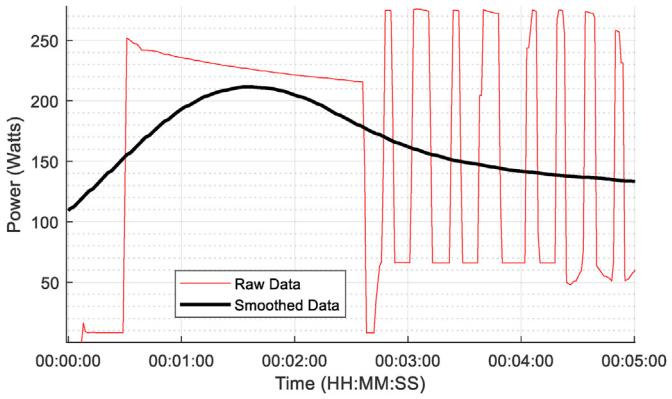

Fig. 7. Power use over the first 5 min of a print.

Table 3
Ender 3 energy use for PLA printed with varying layer heights.

Layer height (um)	Print time (min)	Mean power (W)	Energy per print (kJ)	Volume extruded (cm^3)
100	350	118	2488	26.1
200	226	120	1631	28.6
300	195	110	1296	31.8

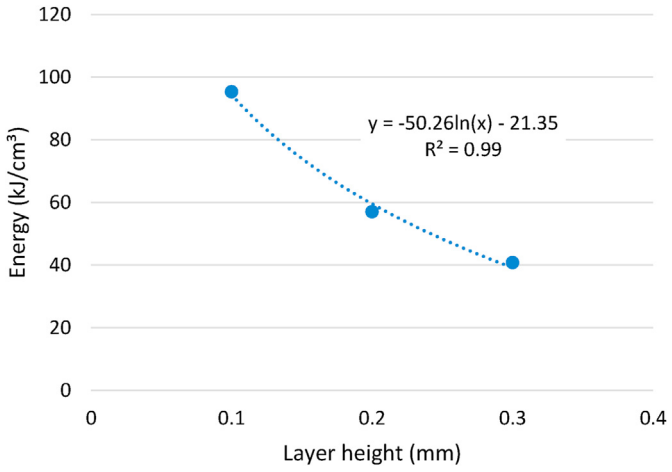

Fig. 8. PLA FFF VSEC vs layer height.

while those for motor, controller and fans will decrease.

This finding indicates that the addition of thermal insulation on the heated bed should be a priority, as it will have a large positive impact with minimal cost. Placing FFF printers in an enclosure will also greatly reduce energy consumption by raising the ambient temperature of the print chamber.

3.1.4. FFF materials comparison

Different materials require different print speeds and temperatures, which will directly affect printer energy use. The print parameters used for a variety of polymers are shown in Table 5.

PLA required the lowest VSEC (Fig. 11). The two materials with the highest bed temperatures (TPU and PA-CF) resulted in the highest energy use. The high bed temperatures were necessary to ensure bonding of the first layer to the build surface and to reduce warping. It is likely that alternative build surfaces, with improved cohesion, would allow lower bed temperatures to be used.

The VSEC values recorded here are much lower than values reported for industrial Stratasys machines of 79.1–1190 kJ/cm^3 (Kellens et al., 2017). This is likely due to the smaller build volumes of desktop machines and the absence of heated enclosures.

Table 4
Non-baseline prints FFF print results.

Print mode	Print time (min)	Mean power (W)	Energy per print (kJ)	Energy comparison with baseline
Baseline	226	120	1631	0%
Insulated bed and hotend	226	92.8	1256	−30%
No heated bed	224	53.1	712.8	−56%
Sequential prints[a]	266	103	1634	0%
100% infill	306	107	1966	+21%
Ghost[b]	218	23.8	312.5	−81%
Multi-colour[c]	311	110	2056	+26%

[a] The printer was allowed to cool down between each print.
[b] The printer was run with the hot end and heated bed turned off.
[c] Printed on a Geeetech A10M.

3.2. Vat polymerisation results

3.2.1. Formlabs Form1+ (SLA) power plots

Fig. 12 shows the power use for the Form1+ printer with 50 μm layers. The smoothed data shows a jump in average power use after 30 min once the base layers were complete. There is also a slow change in average power use over the duration of the print due to the variation in layer curing times.

Inspecting the first 10 min of data (Fig. 13) reveals the printer uses approximately 17 W when the laser is on and 23 W when the motors are moving. The first layer curing time is much longer than subsequent layers to ensure good bonding with the build surface. The laser intensity and speed vary according to the material pre-sets in Preform software, so different materials will result is a slightly different layer curing times.

3.2.2. Anycubic Photon (MSLA) printer power plots

The MSLA printer showed an initial peak in average power due to the longer curing times of the bottom layers (Fig. 14). Subsequently the average power use is flat, as expected with MSLA due to the constant curing times for each layer.

The Photon printer uses approximately 42 W when the UV lights are on and 12 W when off (Fig. 15). Hence energy use for MSLA printers is primarily dependant on layer curing time and the number of layers in the print.

3.2.3. Post-processing

The optional Form wash equipment consumed relatively little energy

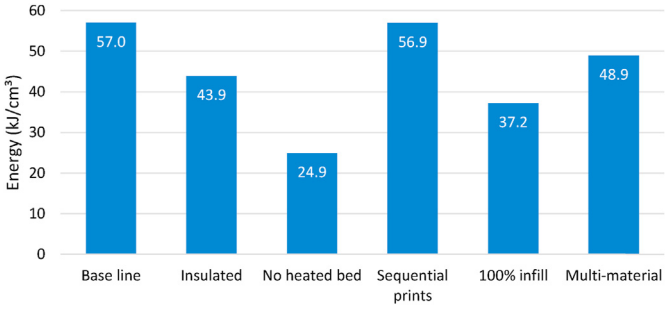

Fig. 9. Comparison of the baseline VSEC vs non-baseline prints.

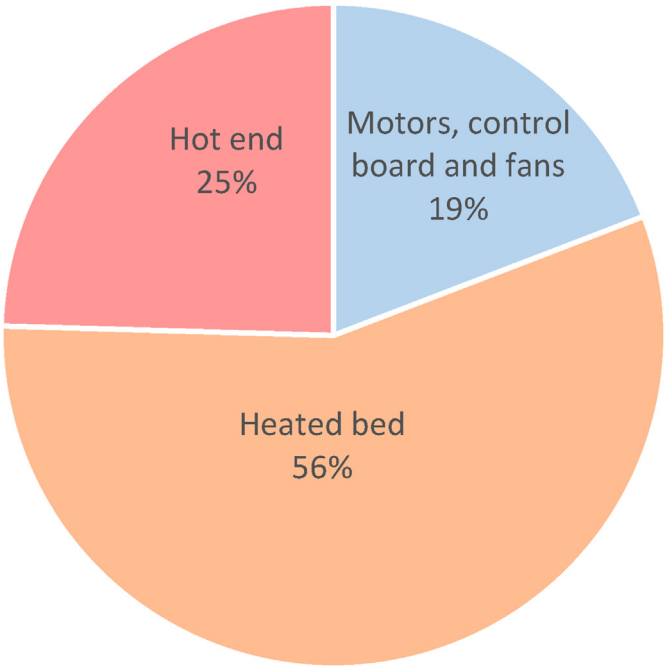

Fig. 10. Breakdown of energy use of the Ender 3 for the baseline print conditions (PLA, 0.2 mm layers).

with a mean power use of 7 W (Fig. 16).

The Form cure uses heating elements and UV lights to fully cure resin parts. The large spikes in power use are likely due to the heating elements as the UV lights are constantly on (Fig. 17).

Total energy used for post-processing a batch of VP parts (washing and curing using Formlabs equipment) is 437 kJ. It is usually possible to fit multiple parts in a batch (depending on part size).

A summary of the results for both the Form1+ and Photon printers are shown in Table 6 and Fig. 18. The Photon used more energy than the Form1+ for most prints despite the fact the Form1+ is a larger printer with a larger build volume.

To reduce the energy use of VP printing the number of layers should be minimised. This can be done by orienting the parts to be closer to the build platform and by increasing the layer heights. Additionally, resins may be chosen that have lower critical energy values (E_C). To minimise the VSEC of MSLA printers, the build plate should be filled as much as possible because the UV lamp uses the same power regardless of how much material is cured in a given layer.

The VSEC values reported here are much lower than equivalent values reported for industrial VP machines of 41.6–124 kJ/cm^3 (Kellens et al., 2017). The reduced energy use is likely due to the smaller machine size and the absence of the resin heaters common in industrial machines.

3.3. Results overview

VP printers use significantly less energy than FFF printers, even when post-processing is included. This aligns well with the theory in section 1.2. However, both AM technologies require significantly higher VSEC values than injection moulding and polymer extrusion (Kent 2008).

Fig. 19 shows the range of VSEC values found for each printer category used in this study, compared to reported values for injection moulding and extrusion.

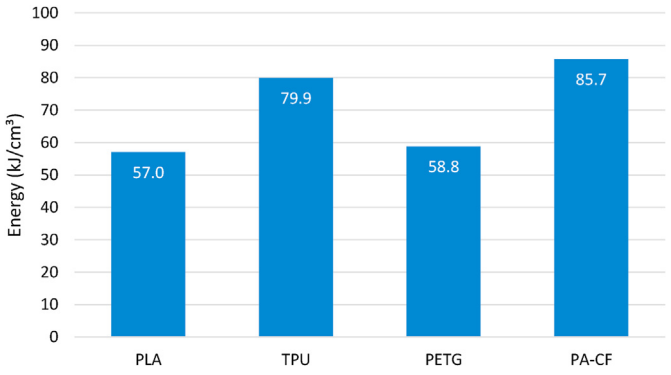

Fig. 11. VSEC for a range of common FFF materials.

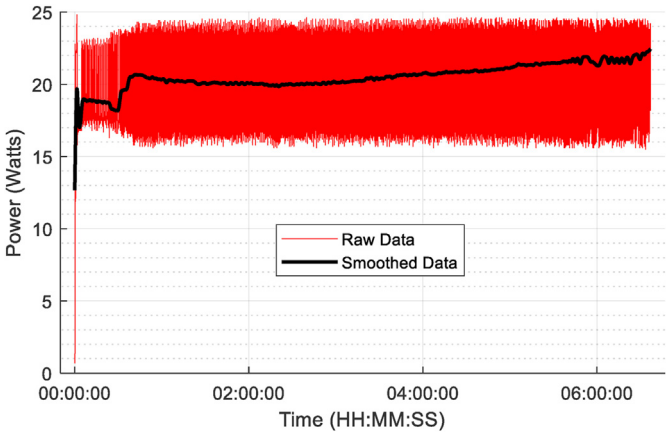

Fig. 12. Form1+ power use over a print (0.05 mm layer height).

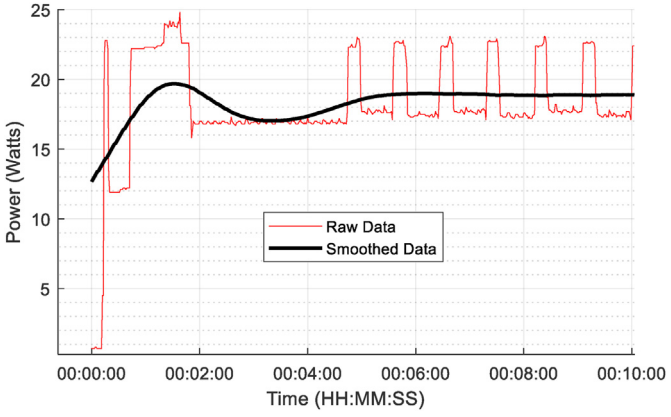

Fig. 13. Form1+ power use over the first 10 min of a print. Layer changes are apparent in the raw data.

Table 5
FFF energy use for a variety of print materials.

Polymer	Hot end temperature (°C)	Heated bed temperature (°C)	Nominal print speed (mm/s)	Print time (min)	Mean power (W)	Energy per print (kJ)
PLA	210	60	50	226	120	1631
TPU	237	80	40	263	149	2365
PETG	245	70	50	232	126	1764
PA-CF	250	90	50	258	162	2451

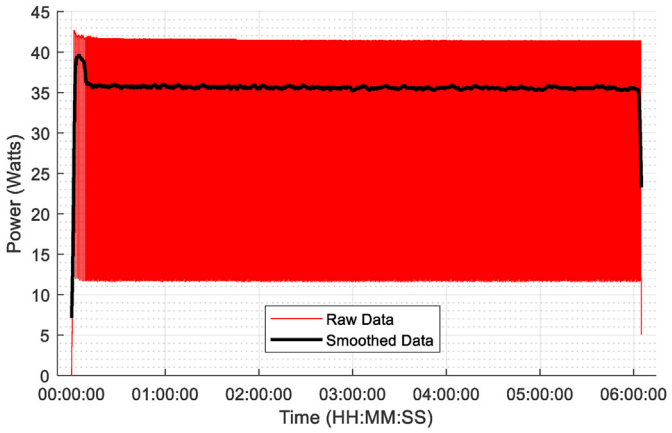

Fig. 14. Photon power use over the duration of a print (0.1 mm layer height).

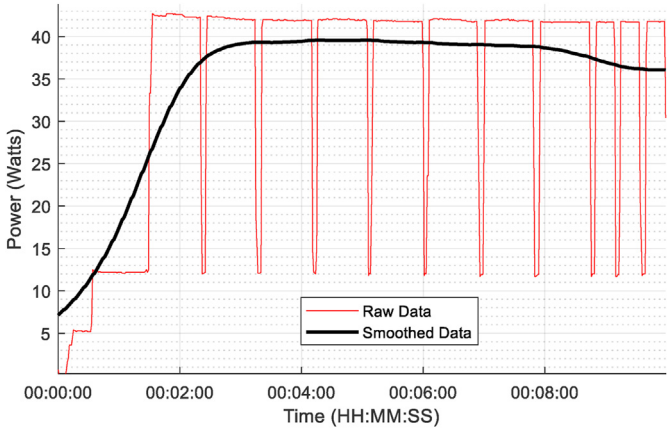

Fig. 15. Anycubic photon power use over first 10 min. Duty cycle of the UV lamp is apparent in the raw data.

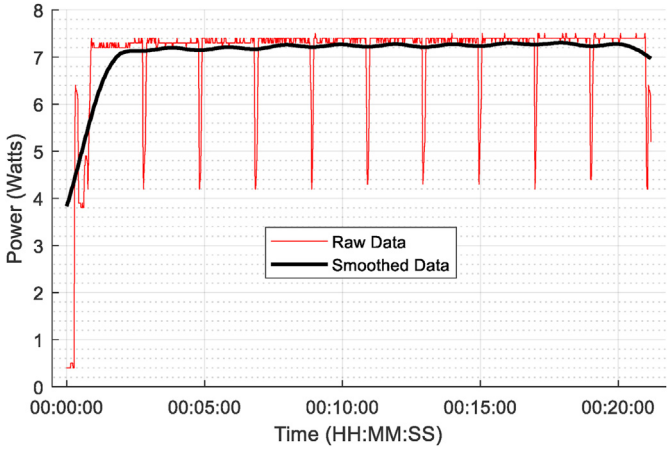

Fig. 16. Power use by Form wash.

4. Predictive energy models

In this section predictive energy models are developed from the empirical data and insights gained from analysing the power-time curves for each printer. A 3D Benchy model (Fig. 20) was used to verify the predictive energy models.

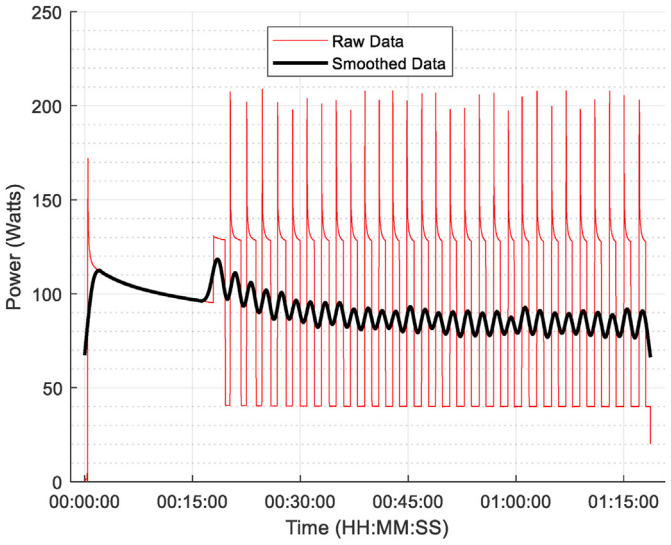

Fig. 17. Power use by Form cure.

Table 6
Energy use for the VP printed parts.

Printer	Layer height (μm)	No. of layers	Volume (cm^3)	Print time (min)	Mean power (W)	Energy (kJ)
Form1+	25	3707	67	800.6	20.7	997.2
	50	1821	67	396.8	20.5	489.6
	100	943	67	233.9	20.1	288
Photon	50	1737	66	438.8	31.9	838.8
	75	1155	66	390.0	34.7	812.9
	100	866	66	364.9	35.6	777.6

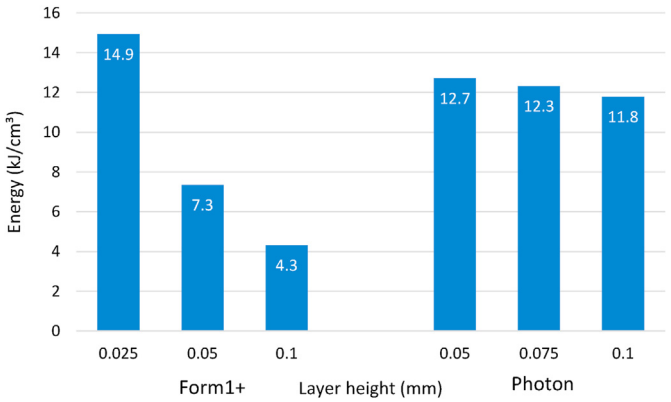

Fig. 18. VSEC for the Form1+ and Photon printers with a range of layer heights.

4.1. FFF energy prediction

Multivariate regression of the experimental data was used to determine print energy, E (kJ), as a function of extruder temperature T_E (°C), bed temperature T_B (°C) and print time t (min).

$$E = -56 + 0.007T_E t + 0.089T_B t \quad (3)$$

Fig. 21 shows the accuracy of Eq. (3) compared to the measured values. The equation was verified by printing a 3D Benchy. The results of the verification tests are shown in orange and show excellent agreement with Eq. (3).

Eq. (3) relies exclusively on temperature parameters and the print

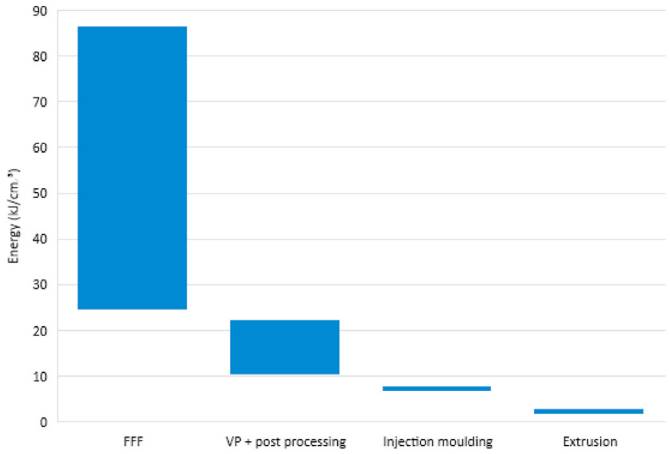

Fig. 19. VSEC values for FFF, VP, injection moulding and extrusion (Kent 2008).

Fig. 20. 3DBenchy model by Creative Tools.

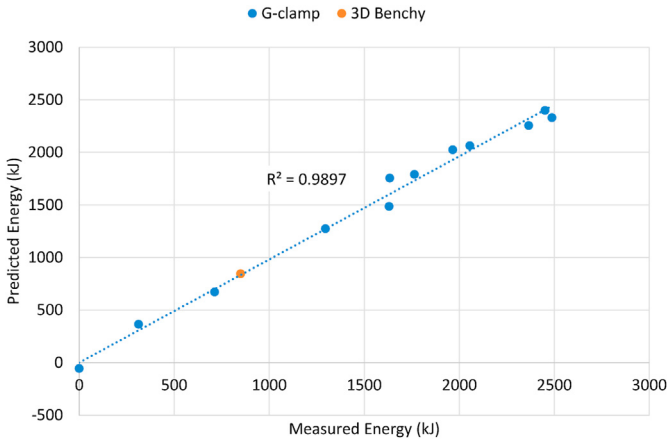

Fig. 21. Predicted vs measured energy using Eq. (3).

time, which are easily known before printing. The equation ought to be accurate for any open frame desktop FFF printer with an uninsulated 235 × 235 mm heated bed.

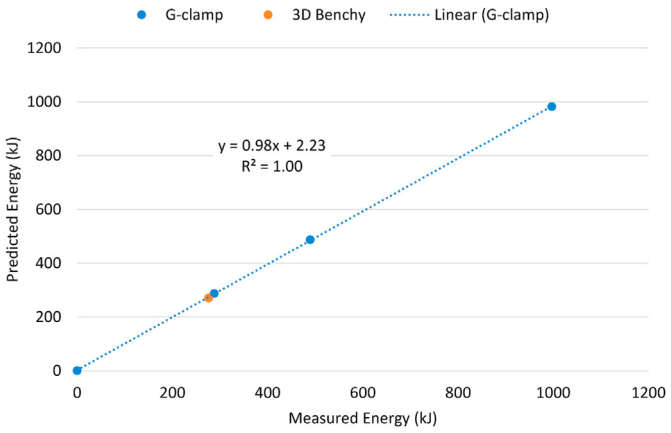

Fig. 22. Predicted vs measured energy use for Form1+ printer using Eq. (4).

4.2. SLA energy prediction

The average power used by the Form1+ varied by only 0.6 W (3%), between the 25 μm and 100 μm prints. Therefore, if variation in power is assumed constant, then energy use becomes a function of print time (Eq. (4)).

$$E = P \times t \tag{4}$$

Estimates of print time are provided by the build preparation software, Preform. Using an empirically determined average value for power (P = 20.4 W), we can compare our calculated energy use against the measured energy use (Fig. 22).

The authors recognise that Eq. (4) may not be accurate for a wide range of materials. This is because the experimentally determined average power values will change slightly due to varying materials settings and print layer times.

4.3. MSLA energy prediction

The power graphs for the Photon printer show the power modulates between two constant power levels. The energy used per print can be calculated by summing the time spent at each energy level (Eq. (5)). This is determined by the layer exposure time and the number of layers required for a given part. The exposure time is an input parameter for the build preparation software, while the number of layers is an output.

$$E = a(Layers_B \times t_B + Layers_T \times t_T) + b(Layers_B + Layers_T) \tag{5}$$

Where a = 41.5 W, b = 11.8 W, $Layers_B$ = no. of bottom layers, t_B = bottom layer exposure time, $Layers_T$ = no. of top layers, t_T = top layer

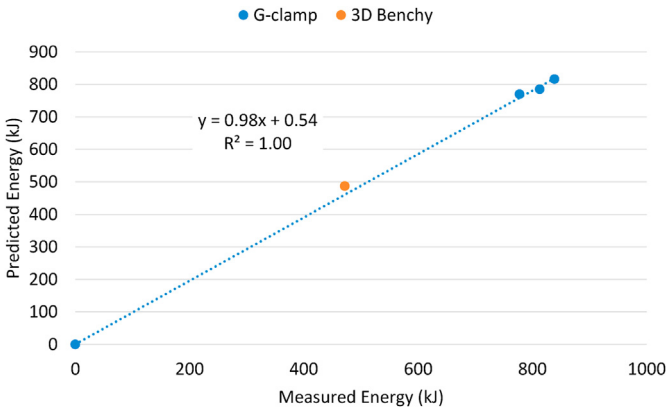

Fig. 23. Calculated energy vs measured energy for the Photon MSLA printer.

exposure time.

Fig. 23 shows how the predicted energy compares to the measured energy.

Eq. (5) will be accurate for any prints made on an unmodified Anycubic Photon printer, as it contains no experimental constants that depend on polymerisation characteristics or part geometries.

5. Conclusion

The volumetric specific energy consumption (VSEC) of parts printed on common desktop 3D printers was measured using a range of build parameters. The VSEC range for FFF was 24.8–85.7 kJ/cm^3, for SLA it was 10.8–21.5 kJ/cm^3 and for MSLA it was 18.4–19.3 kJ/cm^3.

For FFF printers, most of the energy goes into heating the build surface. This is true even for PLA, which requires lower bed temperatures than most materials. Insulating the heated bed and nozzle, printing with low-temperature materials, and printing with large layer heights are all effective methods of reducing the energy use of FFF printers, assuming the part specifications allow it.

The energy use of SLA printers is almost linearly related to print time. Therefore, any actions that reduce print time, such as increasing layer height or reducing the number of print layers, will reduce energy use. For MSLA printers, the energy use is proportional to the layer exposure time, and the number of layers, not the volume of resin being cured. Therefore to lower the VSEC for MSLA printers, the build volume should be as full as possible.

Semi-empirical equations were developed for the three specific 3D printers included in this study. The equations were found to be accurate at predicting the energy required to print a new model with a maximum error of ±3%. The equations will only be accurate for the machines tested but will provide a reasonable estimate for machines with similar components and machine dimensions.

Declaration of competing interest

The authors declare that they have no known competing financial interests or personal relationships that could have appeared to influence the work reported in this paper.

Funding

This work was supported by the University of Central Lancashire, UK (URIP, 2019).

References

3 D Hubs, 2019. 3D Printing Trends - Q1 2019. F. S. Alkaios Bournias-Varotsis.
Baumers, M., Tuck, C., Wildman, R., Ashcroft, I., Rosamond, E., Hague, R., 2013. Transparency built-in. J. Ind. Ecol. 17 (3), 418–431.
Bennett, J., 2017. Measuring UV curing parameters of commercial photopolymers used in additive manufacturing. Addit. Manuf. 18, 203–212.
Dudley, B., 2019. BP Statistical Review of World Energy. London.
International Energy Agency, 2019. World Energy Balances Overview. Online, IEA, p. 793.
Jackson, M.A., Van Asten, A., Morrow, J.D., Min, S., Pfefferkorn, F.E., 2016. A comparison of energy consumption in wire-based and powder-based additive-subtractive manufacturing. Procedia Manuf. 5, 989–1005.
Jacobs, P.F., 1992. Rapid Prototyping & Manufacturing: Fundamentals of Stereolithography. Society of Manufacturing Engineers.
Kearney, A.T., 2018. 3D Printing: Ensuring Manufacturing Leadership in the 21st Century.
Kellens, K., Mertens, R., Paraskevas, D., Dewulf, W., Duflou, J.R., 2017. Environmental impact of additive manufacturing processes: does AM contribute to a more sustainable way of Part Manufacturing? Procedia CIRP 61, 582–587.
Kent, R., 2008. Energy management in plastics processing — framework for measurement, assessment and prediction. Plast., Rubber Compos. 37 (2–4), 96–104.
Khoo, R.Z., Ismail, H., Chow, W.S., 2016. Thermal and morphological properties of poly (lactic acid)/nanocellulose nanocomposites. Procedia Chem. 19, 788–794.
Meteyer, S., Xu, X., Perry, N., Zhao, Y.F., 2014. Energy and material flow analysis of binder-jetting additive manufacturing processes. Procedia CIRP 15, 19–25.
Peng, T., Sun, W., 2017. Energy modelling for FDM 3D printing from a life cycle perspective. Int. J. Manuf. Res. 12 (1), 83–98.
Rejeski, D., Zhao, F., Huang, Y., 2018. Research needs and recommendations on environmental implications of additive manufacturing. Addit. Manuf. 19, 21–28.
Wohlers, T., et al., 2019. 3D Printing and Additive Manufacturing State of the Industry. Wohlers Report 2019, vol. 173. Wohlers Associates Inc. Fort Collins, CO, p. 175.
Yang, Y., Li, L., Pan, Y., Sun, Z., 2017. Energy consumption modeling of stereolithography-based additive manufacturing toward environmental sustainability. J. Ind. Ecol. 21 (S1), S168–S178.
Yoon, H.-S., Lee, J.-Y., Kim, H.-S., Kim, M.-S., Kim, E.-S., Shin, Y.-J., Chu, W.-S., Ahn, S.-H., 2014. A comparison of energy consumption in bulk forming, subtractive, and additive processes: review and case study. Int. J. Precis. Eng. Manuf. Green Technol. 1 (3), 261–279.